

# REFEREE: REFERENCE-AWARE AUDIOVISUAL DEEPFAKE DETECTION

Hyemin Boo\*, Eunsang Lee\*, Jiyoung Lee†

Ewha Womans University, Republic of Korea

## ABSTRACT

Since deepfakes generated by advanced generative models have rapidly posed serious threats, existing audiovisual deepfake detection approaches struggle to generalize to unseen forgeries. We propose a novel reference-aware audiovisual deepfake detection method, called **Referee**. Speaker-specific cues from only one-shot examples are leveraged to detect manipulations beyond spatiotemporal artifacts. By matching and aligning identity-related queries from reference and target content into cross-modal features, **Referee** jointly reasons about audiovisual synchrony and identity consistency. Extensive experiments on FakeAVCeleb, FaceForensics++, and KoDF demonstrate that **Referee** achieves state-of-the-art performance on cross-dataset and cross-language evaluation protocols. Experimental results highlight the importance of cross-modal identity verification for future deepfake detection. The code is available at <https://github.com/ewha-mmai/referee>.

**Index Terms**— Audiovisual deepfake detection, speaker verification

## 1. INTRODUCTION

With the rapid development of generative AI, recent models are increasingly capable of synthesizing media content, including both video and audio. However, this advancement carries a dual nature: while it enables creative and beneficial applications, it also introduces significant risks of misuse and societal harm. The risk has arisen from synthesized media that convincingly imitate humans, known as *deepfake* [1].

The goal of deepfake detection is to distinguish genuine (*i.e.*, real) or spoof (*i.e.*, fake) content. Prior works have relied on a single modality. Image-based approaches have focused on detecting shape distortion [2, 3], boundary artifacts [4, 5, 6], or anomalies in the frequency domain [7, 8] that arise during the synthesis process. On the other hand, audio-based approaches [9, 10] have learned discriminative features to capture vulnerable spectral patterns. Although these methods have shown promising performance, the synthetic contents are generated with higher fidelity, making unimodal detection strategies less reliable. On the other hand, audiovisual deepfake detection [11, 12, 13] has exploited the natural correspondence between facial movements and speech. The dynamic motion patterns [14, 15, 16], such as lip synchronization, or unnatural temporal transitions, have been investigated to capture manipulation cues.

However, such methods often fail when the lips are partially occluded by hands, microphones, or head poses, and their performance further degrades under low-resolution conditions.

When humans encounter a video, they do not fixate on lip motion in isolation; instead, they weave together subtle cues, *e.g.*, tone of voice, facial appearances, and identity coherence, to form a judgment of authenticity. Motivated by this natural ability, we introduce

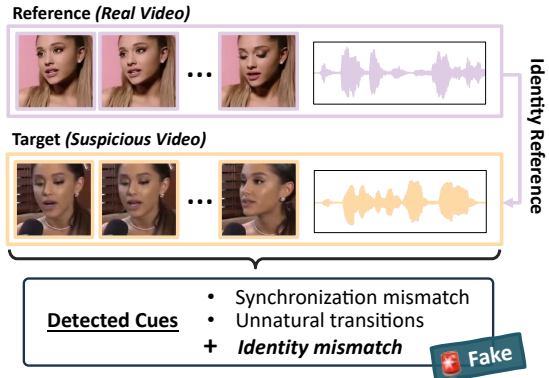


**Fig. 1.** **Referee** introduces robust audiovisual deepfake detection guided by a one-shot reference example, verifying the cross-modal biometrics consistency as well as temporal unnaturalness.

**Referee**, a novel model that examines the consistency of speakers' identity for robust audiovisual deepfake detection. In contrast, artifact-based or synchronization-based methods often rely heavily on the generative models used to create deepfakes in the training set, which limits their generalizability to unseen forgeries [17, 18]. As generative techniques continue to advance, such low-level visual or acoustic artifacts become increasingly subtle or even imperceptible. By comparison, preserving a speaker's unique identity across modalities remains a highly challenging task for generative models. While recent work [19] has proposed a method to measure speaker consistency using contrastive learning, it requires long reference footage (*i.e.*, at least 10 samples of 30 seconds per person), which is often impractical in real-world scenarios.

**Referee** presents an identity bottleneck module (IDB) with learnable identity queries to encode audiovisual sequences into a unified identity representative feature, as shown in Fig. 1. Identity queries obtained from both reference and target content are subsequently aligned through cross-attention to verify speaker identity. This process is optimized by our ID matching loss to ensure that the models can capture speaker-specific cues rather than superficial artifacts. The fused identity representation is then attached to the audiovisual feature, enabling the system to reason jointly about two critical aspects: (1) whether lip-speech synchronization is consistent over time, and (2) whether either or both modalities have been manipulated in a way that violates identity integrity. Finally, the model integrates these signals to classify the content as real or fake. Extensive experiments show **Referee** effectively surpasses current state-of-the-art works on FakeAVCeleb [20], FaceForensics++ [21], and KoDF [22]. It also demonstrates that **Referee** is inherently more resilient to the rapid progress of generative models and better equipped to handle unseen types of deepfakes.

To sum up, our contributions are:

- We propose **Referee**, a reference-aware deepfake detection method that leverages audiovisual correspondence in both

\*Equal contribution. †Corresponding author.

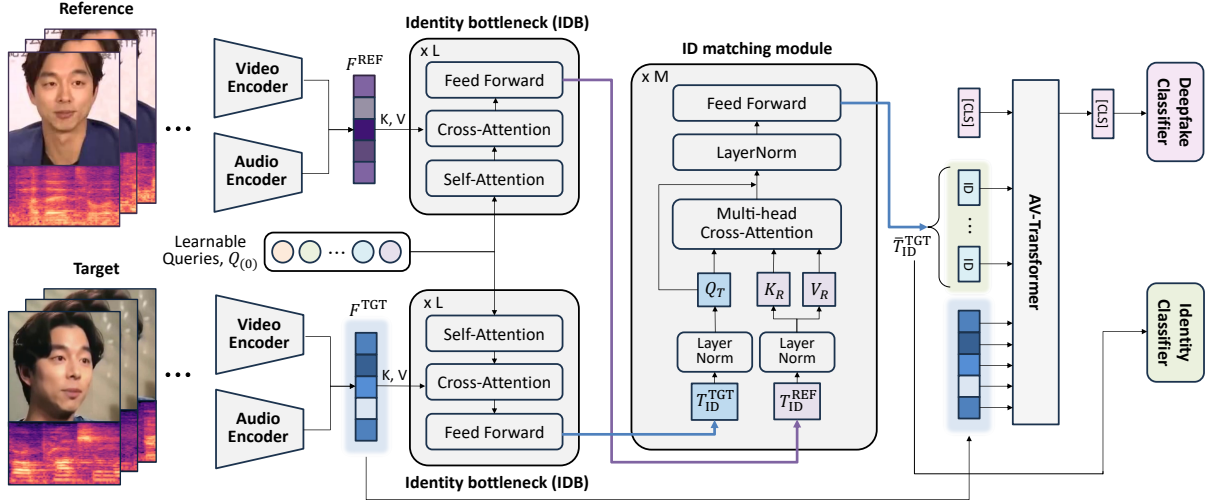


**Fig. 2.** The overall framework of **Referee**. Target and reference videos are encoded into audiovisual features, which are passed through IDB module to generate identity queries. The identity matching module refines the target tokens with respect to the reference tokens, after which the reference-aware identity queries, together with the target audiovisual features and a [CLS] token, are processed by the AV-Transformer for deepfake classification and identity matching.

identity- and temporal-levels.

- **Referee** employs a novel identity bottleneck module with learnable queries and a cross-identity matching mechanism, enabling robust reasoning for audiovisual integrity.
- Extensive experiments on FakeAVCeleb, FaceForensics++, KoDF demonstrate that our **Referee** achieves state-of-the-art performance on both unseen forgery manipulations and cross-lingual evaluation.

## 2. METHOD

### 2.1. Motivation and overview

Most prior approaches [11, 12, 13] for audiovisual deepfake detection have shown impressive performance while concentrating on correct synchronization between audio and video streams. However, there are several challenges: (1) methods relying on synchronization are inherently tied to lip-sync manipulation methodologies, making it difficult to generalize to unseen forgeries. (2) These methods also remain vulnerable under occlusion, low resolution, or degraded signals. To solve these limitations, we propose **Referee** to detect forgery with speaker identity information. We claim that cross-modal biometric cues [23, 24], such as verifying the correspondence between the speaker’s voice and facial appearance, provide a strong basis for deepfake detection.

Given a target and reference video including audio, **Referee** detects subtle identity inconsistencies within the same individual. The proposed method mainly consists of three parts; first, we propose an identity bottleneck module, IDB, to capture the cross-modal identity cues into learnable ID queries. Secondly, identity matching layers learn to check the consistency of speaker identity with the compressed ID query tokens, where the target tokens are re-aligned from the perspective of the reference identity. Finally, the refined ID query is concatenated with the audiovisual feature, and jointly learned within the AV-Transformer to classify the video as real or fake. The overall framework is illustrated in Fig. 2.

### 2.2. Audiovisual feature extraction

Given an input video and audio, our video and audio encoders extract visual and audio features, respectively. In this work, pretrained

audiovisual encoders [25] are used to initialize the parameters. The video and audio are divided into  $N_{seg}$  fixed-length segments of length  $T$  seconds. From each of the  $N_{seg}$  segments, the visual and audio encoders yield segment-level token embeddings. To construct unified representations, these embeddings are concatenated along the temporal axis, forming continuous token sequences for each modality. Formally, this process yields the following visual and audio feature sequences:

$$F_v^* \in \mathbb{R}^{(N_{seg} \cdot T_v) \times D}, \quad (1)$$

$$F_a^* \in \mathbb{R}^{(N_{seg} \cdot T_a) \times D}, \quad (2)$$

where  $*$  denotes either the target (TGT) or reference (REF),  $T_v$  and  $T_a$  denote the number of visual and audio tokens per segment, and  $D$  is the feature dimension.

Finally, for both inputs, the visual and audio sequences are concatenated to form joint audiovisual representations. These are formally expressed as:

$$F^{TGT} = [F_v^{TGT}; F_{mod}; F_a^{TGT}], \quad (3)$$

$$F^{REF} = [F_v^{REF}; F_{mod}; F_a^{REF}], \quad (4)$$

where  $F_{mod}$  is a special learnable token separating the two modalities. These two joint representations,  $F^{TGT}$  and  $F^{REF}$ , serve as the input for subsequent identity reasoning and classification modules.

### 2.3. Identity bottleneck (IDB)

The entanglement of speaker identity with factors like speech content, facial expression, and pose within audiovisual features presents a significant challenge for robust identity (ID) comparison. To address this, we introduce a new ID bottleneck (IDB) that captures ID-related features into a core identity representation.

Inspired by prior works [26, 27], our IDB employs a set of learnable queries to extract and summarize cross-modal identity cues. The module consists of  $L$  identical blocks, each composed of a self-attention layer, a cross-attention layer, and a feed-forward network. The process within each block begins with a set of  $N_q$  learnable identity queries,  $Q_{(0)} \in \mathbb{R}^{N_q \times D}$ . To stabilize learning and encode

relative positions, each query is initialized with a learnable positional embedding. For the  $l$ -th block ( $l = 1, \dots, L$ ), the queries are updated in three stages. At each block, the queries first undergo self-attention, allowing them to capture internal dependencies and integrate information among themselves. The resulting intermediate queries,  $\tilde{Q}_{(l)}$ , then act as the query input to a multi-head cross-attention layer, where the joint representation ( $F^{\text{TGT}}$  or  $F^{\text{REF}}$ ) serves as the key and value. The output of the cross-attention layer is passed through a feed-forward network to produce the block’s final output,  $Q_{(l)}$ . This three-stage update process is formally defined as:

$$\tilde{Q}_{(l)} = \text{SA}(\text{LN}(Q_{(l-1)})) + Q_{(l-1)}, \quad (5)$$

$$\hat{Q}_{(l)} = \text{CA}(\text{LN}(\tilde{Q}_{(l)}), \text{LN}(F)) + \tilde{Q}_{(l)}, \quad (6)$$

$$Q_{(l)} = \text{FFN}(\text{LN}(\hat{Q}_{(l)})) + \hat{Q}_{(l)} \quad (7)$$

Repeating this three-stage process over  $L$  blocks progressively refines the queries into tokens that encode essential identity information. This yields two distinct sets of identity tokens:  $T_{\text{ID}}^{\text{TGT}} = Q_{(L)}^{\text{TGT}} = \text{IDB}(F^{\text{TGT}})$  from the target features, and  $T_{\text{ID}}^{\text{REF}} = Q_{(L)}^{\text{REF}} = \text{IDB}(F^{\text{REF}})$  from the reference features.

#### 2.4. Deepfake detection

**Referee** performs deepfake detection by jointly leveraging fine-grained audiovisual correspondence cues and identity consistency information between the target and the reference. Our ID matching module aggregates and compares identity consistency, which employs  $M$  stacked cross-attention blocks. The target tokens serve as the query, while the reference tokens act as the key and value. Namely, the target query  $T_{\text{ID}}^{\text{TGT}}$  is refined by conditioning it on the  $T_{\text{ID}}^{\text{REF}}$ . This matching process generates reference-aware identity tokens,  $\bar{T}_{\text{ID}}^{\text{TGT}}$ , which not only retain the intrinsic identity characteristics of the target but also embed information about similarities and discrepancies with the reference. As a result, even subtle inconsistencies between the two identities can be amplified and clearly manifested in the final representation.

Subsequently,  $\bar{T}_{\text{ID}}^{\text{TGT}}$  are concatenated with the [CLS] token and the target audiovisual features  $F^{\text{TGT}}$ :

$$X^{\text{TGT}} = [T_{\text{CLS}}; \bar{T}_{\text{ID}}^{\text{TGT}}; F^{\text{TGT}}]. \quad (8)$$

The resulting sequence  $X^{\text{TGT}}$  is passed through joint audiovisual transformer blocks (shortly, AV-Transformer), which integrate temporal audiovisual factors (e.g., artifacts, synchronization cues) with identity-centric cues. To better distinguish different token roles, we incorporate type embeddings that explicitly encode whether a token corresponds to the classification token or identity queries. This role-specific bias encourages the model to facilitate distinct representations following their roles. Finally, a deepfake classifier takes the [CLS] token, which produces the final deepfake prediction.

To ensure the ID matching module produces highly discriminative features for identity consistency check, we design an auxiliary identity verification task. Specifically, the reference-aware identity tokens  $\bar{T}_{\text{ID}}^{\text{TGT}}$  are aggregated via average pooling to form a single feature vector. This vector is then fed into a dedicated MLP head to predict the identity matching logit,  $Y_{\text{ID}}$ . This auxiliary objective encourages the matching module to learn features that are not only useful for the final deepfake detection task but also explicitly optimized for robust identity verification.

Our overall training objective is composed of a deepfake classification loss  $\mathcal{L}_{\text{RF}}$  and an identity matching loss  $\mathcal{L}_{\text{ID}}$ , both implemented as a standard cross-entropy loss. The identity matching task verifies

Method	Modality	ACC	AUC
Xception [21]	V	67.9	70.5
LipForensics [28]	V	80.1	82.4
FTCN [29]	V	64.9	84.0
CViT [30]	V	69.7	71.8
RealForensics [31]	V	89.9	94.6
VFD [32]	AV	81.5	86.1
AVoID-DF [16]	AV	83.7	89.2
AVFF [14]	AV	98.6	99.1
<b>Referee</b>	<b>AV</b>	<b>99.24</b>	<b>99.71</b>

**Table 1.** Intra-dataset comparison of different unimodal (V) and multimodal (AV) methods on FakeAVCeleb.

Method	Train set	Modality	AUC	AP
LipForensics [28]	FF++	V	<b>93.25</b>	-
RealForensics [31]	FF++/AVLips	V	91.32	-
Xception [21]†	FakeAVCeleb	V	58.83	80.09
LipFD [12]†	FakeAVCeleb	AV	53.43	78.12
AVAD [33]‡	LRS2/LRS3	AV	38.19	67.40
<b>Referee</b>	FakeAVCeleb	<b>AV</b>	<b>68.44</b>	<b>87.10</b>

**Table 2.** Cross-dataset performance comparison on FF++. † denotes the reimplemented results based on their official code. ‡ tests on the publicly available trained weights.

whether two videos contain the same identity. Regardless of whether the manipulation originates from the reference speaker, we treat the forged content as representing another identity. Equivalently, pairs were labeled as the same identity only if they came from distinct real recordings of the same individual.

By jointly learning the deepfake classification and the identity matching tasks, the model not only learns to detect whether an input video is manipulated but also acquires the ability to discriminate identities. This identity discrimination capability, in turn, enhances the effectiveness of deepfake detection.

## 3. EXPERIMENTS

### 3.1. Datasets

**FakeAVCeleb.** We train **Referee** on FakeAVCeleb [20], which includes both audio and visual manipulations. Visual manipulations were created using FaceSwap [34], FSGAN [35], and Wav2Lip [36], while audio manipulations were generated with SV2TTS [37]. The dataset provides deepfake videos with only visual manipulation, only audio manipulation, or manipulations in both modalities. We further sourced 37k real videos corresponding to the same 500 identities from VoxCeleb2 [38] to use as reference videos.

**FaceForensics++ (FF++).** We use FF++ [21] to evaluate the generalization capabilities of methods across the difference of training and test data. The benchmark encompasses five manipulation methods: DeepFakes [39], FaceSwap [34], Face2Face [40], NeuralTexture [41], and FaceShift [42]. It includes data subjected to not only face swapping but also expression manipulation, enabling the evaluation of the models’ performance across diverse manipulation types. In the official test split, we only use the videos from which the corresponding audio tracks could be reliably extracted.

**KoDF.** To evaluate the performance on zero-shot cross-lingual forgery detection, we utilize KoDF [22], a large-scale deepfake

Method	Modality	AUC	AP
Xception [21]	Yellow	77.7	76.9
LipForensics [28]	Yellow	86.6	89.5
FTCN [29]	Yellow	68.1	66.8
RealForensics [31]	Yellow	93.6	95.7
AV-DFD [13]	AV	82.1	79.6
AVAD [33]	AV	86.9	87.6
AVFF [14]	AV	95.5	93.1
<b>Referee</b>	<b>AV</b>	<b>97.5</b>	<b>98.1</b>

**Table 3.** Cross-dataset performance comparison on KoDF.

dataset based on Korean speech generated using six different techniques: FaceSwap [34], DeepFaceLab [43], FSGAN [35], FOMM [44], ATFHP [45], and Wav2Lip [36]. Following [33, 14], we randomly sampled 100 real and 100 audio-driven manipulated fake videos for evaluation, except manipulation techniques already employed in FakeAVCeleb.

### 3.2. Implementation details and evaluation setup

Audiovisual encoder is initialized on Synchformer [25] pretrained on LRS3 [46]. Videos are sampled at 25 fps, while audio is sampled at 16 kHz and converted into 128-channel mel-spectrograms with 25 ms windows and a 10 ms hop. From each video, we extract a sequence of 8 overlapping segments with a duration of 0.64s (16 frames). The weighted sampling is adopted during training, while the network is optimized by Adam with 1e-5 learning rate. The learning rate is managed by a cosine annealing scheduler, which includes a linear warmup and decays to a minimum rate of 1e-6. During training, references are randomly sampled from real videos of the same identity, while evaluation uses predefined target-reference pairs. Importantly, the reference videos employed for training and testing are strictly disjoint to avoid data leakage. For evaluation, each video is divided into consecutive 2.88s windows with a 5% temporal overlap. The final video-level prediction is obtained by averaging the softmax probabilities across windows, followed by an argmax operation. Our code will be released upon acceptance.

Following previous works [12, 14], we assess the performance using accuracy (ACC), average precision (AP), and the area under the ROC curve (AUC). While ACC provides an intuitive measure of overall correctness but can be misleading under severe class imbalance, such as FakeAVCeleb, which contains 500 real and 21,066 fake videos. To address this issue, we additionally employ AP and AUC, both of which are threshold-independent. By using these three metrics, we can more reliably and comprehensively compare model performance, regardless of class imbalance within the dataset.

### 3.3. Results

**Intra-dataset.** Following prior works [16, 14], FakeAVCeleb is split 70% for training, and 30% for a test set. Table 1 shows that our method achieves superior improvements over visual-only and audio-visual baselines. Compared to RealForensics, the strongest visual model, our approach achieves gains of 9.3%p in ACC and 5.1%p in AUC, demonstrating the limitation of relying solely on visual cues. While audiovisual detectors such as AVFF already surpass unimodal approaches, our **Referee** achieves SoTA with additional gains of 0.6%p in ACC, and 0.6%p in AUC. It demonstrates that, beyond simple multimodal fusion, explicitly modeling cross-modal biometrics consistency allows our approach to capture subtle discrepancies that current SoTA models miss.

Method	ACC	AUC	AP
w/o reference identity query	99.03	99.33	99.98
w/o identity matching loss	<u>99.09</u>	<u>99.69</u>	<b>99.99</b>
<b>Referee</b>	<b>99.24</b>	<b>99.71</b>	<b>99.99</b>

**Table 4.** Effectiveness of the identity matching design.

# Query Tokens	CA Layers	ACC	AUC	AP
4	1	99.06	98.90	99.96
4	2	<u>99.15</u>	<u>98.96</u>	<u>99.96</u>
6	2	<b>99.24</b>	<b>99.71</b>	<b>99.99</b>

**Table 5.** Performance varying the number of identity query tokens, and cross-attention layers.

**Cross-dataset.** We evaluate the generalization ability of our method in a cross-dataset setting, where the model is trained solely on FakeAVCeleb and tested on unseen datasets without any finetuning. As reported in Table 2, **Referee** outperforms all cross-dataset evaluated models in terms of both AUC and AP, demonstrating strong robustness to distribution shifts and unseen manipulation methods. Following the protocol from [33, 14], Table 3 validates cross-lingual robustness, where our method achieves 97.5% AUC and 98.1% AP, surpassing previous SoTA results by more than 2%p in AUC and over 5%p in AP. It demonstrates that **Referee** shows consistent robustness to both zero-shot cross-lingual forgery and unseen manipulation methods. Overall, the results highlight the advantage of incorporating identity-aware representations, which enable our approach to mitigate the overfitting to dataset-specific artifacts observed in prior works.

**Ablation study.** Table 4 examines the effectiveness of the identity matching design. The removal of reference identity query leads to a noticeable drop in both ACC and AUC. This result highlights the necessity of our modeling reference-guided identity consistency. In contrast, when the identity matching module is retained but the identity loss is excluded, performance remains strong but slightly lower than the full model. This result indicates that our auxiliary matching task improves the robustness. These findings confirm that both the structural design of the ID matching module and its dedicated loss function are crucial for achieving optimal performance. Table 5 reports the performance varying the number of query tokens and cross-attention (CA) layers while keeping the IDB layers at two. Increasing the number of CA layers consistently improves performance across all metrics. While keeping the CA layers at two, expanding the number of query tokens from 4 to 6 yields a further performance gain, achieving the best overall results. While increasing the number of layers and queries further improves performance, we observe a clear trade-off with computational cost. This suggests that our chosen configuration strikes a favorable balance between accuracy and efficiency.

## 4. CONCLUSION

We introduce **Referee**, the reference-aware audiovisual framework that explicitly leverages a reference video for robust deepfake detection. Our identity bottleneck module implicitly learns cross-modal biometrics in ID queries for speaker verification. This identity-guided reasoning enables the model to move beyond superficial artifacts, offering stronger generalization to unseen manipulations and making it a resilient solution against the rapid progress of generative forgeries.

## 5. REFERENCES

- [1] R. Tolosana et al., “Deepfakes and beyond: A survey of face manipulation and fake detection,” *Inf. Fusion*, 2020.
- [2] H. Guo, , et al., “Eyes tell all: Irregular pupil shapes reveal gan-generated faces,” in *ICASSP*, 2022.
- [3] Y. Li et al., “Exposing deepfake videos by detecting face warping artifacts,” *arXiv preprint arXiv:1811.00656*, 2018.
- [4] L. Li et al., “Face x-ray for more general face forgery detection,” in *CVPR*, 2020.
- [5] H. Chen et al., “Watching the big artifacts: Exposing deepfake videos via bi-granularity artifacts,” *PR*, 2023.
- [6] X. Fu et al., “Faces blind your eyes: Unveiling the content-irrelevant synthetic artifacts for deepfake detection,” *IEEE TIP*, 2025.
- [7] C. Tan et al., “Frequency-aware deepfake detection: Improving generalizability through frequency space domain learning,” in *AAAI*, 2024.
- [8] J. Li et al., “Frequency-aware discriminative feature learning supervised by single-center loss for face forgery detection,” in *CVPR*, 2021.
- [9] A. Qais et al., “Deepfake audio detection with neural networks using audio features,” in *ICICCS*, 2022.
- [10] N. Chakravarty et al., “A lightweight feature extraction technique for deepfake audio detection,” *Multimed. Tools Appl.*, 2024.
- [11] S. Agarwal et al., “Detecting deep-fake videos from phoneme-viseme mismatches,” in *CVPRW*, 2020.
- [12] W. Liu et al., “Lips are lying: Spotting the temporal inconsistency between audio and visual in lip-syncing deepfakes,” *NeurIPS*, 2024.
- [13] Y. Zhou et al., “Joint audio-visual deepfake detection,” in *ICCV*, 2021.
- [14] T. Oorloff et al., “Avff: Audio-visual feature fusion for video deepfake detection,” in *CVPR*, 2024.
- [15] Y. Liang et al., “Speechforensics: Audio-visual speech representation learning for face forgery detection,” *NeurIPS*, 2024.
- [16] W. Yang et al., “Avoid-df: Audio-visual joint learning for detecting deepfake,” *TIFS*, 2023.
- [17] D. Cozzolino et al., “Id-reveal: Identity-aware deepfake video detection,” in *ICCV*, 2021.
- [18] X. Dong et al., “Protecting celebrities from deepfake with identity consistency transformer,” in *CVPR*, 2022.
- [19] D. Cozzolino et al., “Audio-visual person-of-interest deepfake detection,” in *CVPR*, 2023.
- [20] H. Khalid et al., “Fakeavceleb: A novel audio-video multimodal deepfake dataset,” *NeurIPS*, 2021.
- [21] A. Rossler et al., “Faceforensics++: Learning to detect manipulated facial images,” in *ICCV*, 2019.
- [22] P. Kwon et al., “Kodf: A large-scale korean deepfake detection dataset,” in *ICCV*, 2021.
- [23] A. Nagrani et al., “Seeing voices and hearing faces: Cross-modal biometric matching,” in *CVPR*, 2018.
- [24] J. Lee et al., “Imaginary voice: Face-styled diffusion model for text-to-speech,” in *ICASSP*, 2023.
- [25] V. Iashin et al., “Synchformer: Efficient synchronization from sparse cues,” in *ICASSP*, 2024.
- [26] A. Jaegle et al., “Perceiver io: A general architecture for structured inputs & outputs,” in *ICLR*, 2021.
- [27] J. Li et al., “Blip-2: Bootstrapping language-image pre-training with frozen image encoders and large language models,” in *ICML*, 2023.
- [28] A. Haliassos et al., “Lips don’t lie: A generalisable and robust approach to face forgery detection,” in *CVPR*, 2021.
- [29] Y. Zheng et al., “Exploring temporal coherence for more general video face forgery detection,” in *ICCV*, 2021.
- [30] D. Wodajo et al., “Deepfake video detection using convolutional vision transformer,” *arXiv preprint arXiv:2102.11126*, 2021.
- [31] A. Haliassos et al., “Leveraging real talking faces via self-supervision for robust forgery detection,” in *CVPR*, 2022.
- [32] H. Cheng et al., “Voice-face homogeneity tells deepfake,” *TOMM*, 2023.
- [33] C. Feng et al., “Self-supervised video forensics by audio-visual anomaly detection,” in *CVPR*, 2023.
- [34] M. Kowalski, “Faceswap,” <https://github.com/MarekKowalski/FaceSwap/>, 2018, Accessed: 2025-09-09.
- [35] Y. Nirkin et al., “Fsgan: Subject agnostic face swapping and reenactment,” in *ICCV*, 2019.
- [36] K. Prajwal et al., “A lip sync expert is all you need for speech to lip generation in the wild,” in *ACM MM*, 2020.
- [37] Y. Jia et al., “Transfer learning from speaker verification to multispeaker text-to-speech synthesis,” *NeurIPS*, 2018.
- [38] J. S. Chung et al., “Voxceleb2: Deep speaker recognition,” in *Interspeech*, 2018.
- [39] Deepfakes, “faceswap,” <https://github.com/deepfakes/faceswap>, 2018, Accessed: 2025-09-09.
- [40] J. Thies et al., “Face2face: Real-time face capture and reenactment of rgb videos,” in *CVPR*, 2016.
- [41] J. Thies et al., “Deferred neural rendering: Image synthesis using neural textures,” *ACM TOG*, 2019.
- [42] L. Li, Bao, et al., “Faceshifter: Towards high fidelity and occlusion aware face swapping,” *arXiv preprint arXiv:1912.13457*, 2019.
- [43] I. Perov et al., “Deepfacelab: Integrated, flexible and extensible face-swapping framework,” *arXiv preprint arXiv:2005.05535*, 2020.
- [44] A. Siarohin et al., “First order motion model for image animation,” *NeurIPS*, 2019.
- [45] R. Yi et al., “Audio-driven talking face video generation with learning-based personalized head pose,” *arXiv preprint arXiv:2002.10137*, 2020.
- [46] T. Afouras et al., “Lrs3-ted: a large-scale dataset for visual speech recognition,” *arXiv preprint arXiv:1809.00496*, 2018.